An Interactive MATLAB Program for Fitting Transfer Functions to Frequency Responses

Jared A. Grauer*

NASA Langley Research Center, Hampton, Virginia, 23681

A computer program called FRFit (Frequency Response Fitting) is described for fitting single-input single-output transfer function models to empirical frequency response data. The program is interactive in that the user specifies "elementary factors" (gain, delay, pure differentiators and integrators, and first- and second-order zeros and poles) by entering numerical values or moving sliders in a graphical user interface. A nonlinear optimization can then be performed to obtain maximum likelihood estimates of transfer function parameters and uncertainties to provide feedback on the modeling and refine estimates. Several examples are discussed, including the identification of aircraft pitch dynamics from simulation data and data reported in the literature, approximating Theodorsen's function of unsteady aerodynamics, and obtaining a reduced-order model of a computational fluid dynamics code describing the unsteady aerodynamics around an aeroelastic wing. The program has some usefulness as a teaching aid, and can be applied to model structure determination, reduced-order modeling, preliminary analysis, and simple system identification problems. The program was written in MATLAB® and is planned for public release through the NASA Software Catalog.

I. Nomenclature

cov(.)	=	covariance operator
ln	=	natural logarithm
j	=	imaginary number, = $\sqrt{-1}$
$\Re$	=	real part of number
s	=	Laplace variable
σ	=	real part of number
ω	=	radian frequency, rad/s
$_0$	=	starting value
$\hat{}$	=	estimate
*	=	complex conjugate
†	=	complex conjugate transpose
^{T}	=	transpose
$^{-1}$	=	matrix inverse
$\bar{}$	=	average value

*Research Engineer, Dynamic Systems and Control Branch, MS 308, Associate Fellow AIAA.

II. Introduction

When tasked with identifying a state-space model of a multiple-input multiple-output system for which little physical insight into a model structure was known (see the full discussion in Ref. [1]), the present author began by examining individual single-input single-output frequency responses to infer a mathematical model of the system (model structure determination) and obtain values of constants in the model (parameter estimation). Transfer function models would then be combined into a larger state-space model to be estimated all at once using the multiple inputs and multiple outputs [2].

Although several software packages have been developed for fitting models to frequency response data, e.g., those described in Refs. [3–5], it became apparent that many of the available tools had perceived shortcomings in regard to completing this task, such as being proprietary, too costly, too large a program to efficiently run on many smaller problems, not parameterizing transfer functions in an intuitive manner for model structure determination, or being batch processed instead of interactive.

As such, it was deemed worthwhile to write a new computer program with the following attributes. The program should have the single purpose of fitting single-input single-output transfer functions to empirical frequency response data. This would decrease the program complexity, enable an efficient analysis, and decouple the model structure determination and parameter estimation from other parts of the analysis, such as computing the frequency response data from measured time histories. The program should be written in MATLAB® (The MathWorks Inc., Natick, Massachusetts) to integrate the program with other analysis tools and not work as a standalone application. A graphical user interface, where the analyst can add, remove, or modify transfer function "elementary factors" (gain, delay, integrators and differentiators, and first- and second-order zeros and poles) quickly using buttons, sliders, and edit fields is important. As mentioned in Ref. [6],

> Interactive programs are generally reserved for difficult problems, where the approach to the solution is not clear at the outset. The solution progress tends to be discontinuous and incremental, with numerous dead ends met during the process.

As model structure determination can be an iterative process, having the ability to change the model and see the effects in real time would significantly help an analyst working on difficult problems. The parameterization of the transfer function in this form adds some complexity to the parameter estimation process, but uses the analyst's intuition and knowledge of how these factors change the frequency response. Lastly, the program should have some capability to refine the manually-tuned coefficients of the model, providing optimized parameters, uncertainties, statistical metrics of the fit, and some feedback regarding the postulated model structure

This paper describes the form and function of the program developed with these attributes, called FRFit (Frequency Response Fitting). The program was written using the MATLAB® App Designer and is called from the command prompt. The analyst interactively builds and tunes a transfer function model to fit frequency response data, and a nonlinear optimization can be run to obtain maximum likelihood parameter estimates and uncertainties. The program is limited to examining single-input single-output frequency responses and estimating transfer functions, which are relatively simple system identification problems. However, this information can be used to to gain insight into a system or data, and can be later refined with other more general, robust, and advanced identification tools [2, 3, 7]. Therefore, this program is particularly useful for determining reduced-order models or models for which little physical insight is available for the system. The software could also be used as a teaching aid, or for refreshing knowledge of transfer functions and frequency responses. The program can be re-engineered and adapted from this description, or it is planned to be released through the NASA Software Catalog [8].

The discussion is hereafter organized as follows. Section III gives a theoretical background on the subject material. Section IV summarizes some techniques for fitting transfer function models to frequency response data, both state of the art and standard practices. Section V introduces the FRFit program. Section VI presents four examples of results obtained using FRFit.

III. Theoretical Background

A transfer function $H(s)$ is a frequency-domain representation of the dynamics between an input and an output for a linear time-invariant (LTI) system. The argument $s = \sigma + j\omega$ is the complex-valued Laplace variable. Transfer functions are typically expressed as a ratio of polynomials of s, in some factorization, or as a partial fraction expansion.

The frequency response of a transfer function quantifies the steady-state amplitude and phase modulation between the input and output as a function of frequency. The frequency response is obtained from a transfer function by setting

$\sigma = 0$ and evaluating $H(j\omega)$. The frequency response is complex valued, and can be written in rectangular coordinates or polar coordinates as

$$H(j\omega) = H_R(j\omega) + H_I(j\omega)j \tag{1a}$$
$$= |H(j\omega)|\, e^{j\angle H(j\omega)} \tag{1b}$$

respectively, where the subscripts $_R$ and $_I$ indicate the real and imaginary components, and where

$$|H(j\omega)| = \sqrt{H_R^2(j\omega) + H_I^2(j\omega)} \tag{2}$$
$$\angle H(j\omega) = \arctan\left[\frac{H_I(j\omega)}{H_R(j\omega)}\right] \tag{3}$$

are the magnitude and phase. Although defined for steady-state oscillation, the frequency response nonetheless provides a complete description of the LTI dynamics between the input and output.

The frequency response is often visualized as a Bode plot, where the magnitude and phase components are shown as a function of frequency with units dB and deg, respectively. Frequency responses are also sometimes visualized as a Nichols chart, where the Bode magnitude is plotted against the Bode phase, or as a Nyquist plot, where the frequency response real and imaginary parts are plotted against each other.

Frequency responses can also be obtained empirically, from measured input and output data, without an analytic transfer function. One technique, called the frequency approach [9], is to excite an input with a sinusoid, compare the steady-state magnitude and phase to the input, and repeat this process for many frequencies over the bandwidth of interest. Another approach, called the Fourier approach [10], is to excite the system with shorter inputs, such as pulses or doublets, and compute the frequency response from ratios of input and output Fourier transform data. A recent technique combined the frequency and Fourier approaches using multisine inputs to efficiently excite multiple-input, multiple-output systems [11, 12]. Another technique is the spectral approach [13], where spectral densities are estimated and then combined to produce the frequency response. In some applications, the Eigensystem realization algorithm (ERA) can be used to extract impulse responses, which can then be transformed into frequency responses [14, 15]. An overview of standard techniques is given in Ref. [16].

IV. Historical Perspective

Given empirical data for a frequency response, it is possible to infer the structure of a transfer function describing that data and estimate model parameters. Indeed, a graphical approach for quickly plotting asymptotes of the frequency response was the motivation for developing the Bode plot [17]. This was often done by the use of "elementary factors" — gains, differentiators and integrators, and first- and second-order poles and zeros. These factors have relatively simple and well-known frequency response characteristics, and were combined to match empirical frequency response data. References [17, 18] provide stencils for doing this with frequency responses that have been normalized over frequency.

Reference [19] suggests an iterative procedure where elementary factors are sequentially added. Based on the differences between the frequency response data and the current model, displayed as a Bode plot, additional factors are added. The process is stopped when the differences are less than specified threshold values. It was suggested that factors be added in the following order: gains, differentiators or integrators, first-order poles or zeros, and second-order poles or zeros. This process is similar to other interactive system identification techniques such step-wise regression [7, 20, 21].

After a model structure has been decided upon, values of model parameters within the transfer function can be estimated to best match the data. Reference [22] developed a least-squares technique for doing this. This technique was also extended for the case when input and output Fourier transform data are available [23]. Iterative techniques were developed that usually overcome inaccuracies of the least-squares technique when the data spanned several decades of frequency or when the denominator had large fluctuations [24]. The methods of Refs. [22, 24] are included in the Signal Processing Toolbox™ and System Identification Toolbox™. The transfer function model used in these algorithms is a ratio of polynomials, where the user selects the order of the polynomials. System models, based either on transfer functions or state-space models, can be identified using the software package called CIFER®, as well as many other aircraft system identification procedures and utilities [3].

V. FRFit Program Overview

A. General View

The FRFit program is called from the MATLAB® command prompt with two inputs: a vector of n_ω frequencies in rad/s, and a vector of the complex-valued frequency responses at those frequencies. The program window, shown in Fig. 1, then opens. It is also possible to call the function with an initial model parameters and uncertainties, to more quickly populate a model or to provide prior information or hold some values fixed during the optimization, as discussed below.

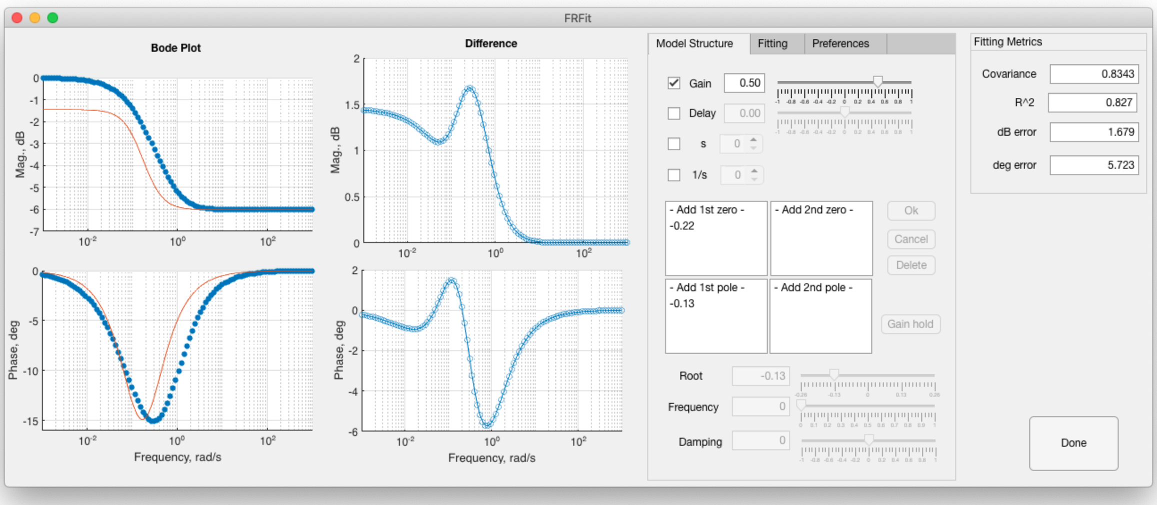

Fig. 1 FRFit program window.

The tabbed group to the far left contains the visualization of the frequency response and the differences. For the Bode plots shown in Fig. 1, there is a left column for the Bode plot, where the data are blue dots and the model is the red line. The model is computed over a fine frequency grid over the bandwidth of interest, in addition to at the frequencies in the data, to allow an accurate visualization of the frequency response in addition to comparing the model to the data points. The column to the right illustrates the Bode magnitude and phase differences between the model and the frequency response data. This information can also be plotted using real and imaginary parts of the frequency response, or as a Nichols chart.

In the tabbed group to the right, the "Model Structure" tab allows the user to manually tune the transfer function model. The model is parameterized in the form

$$\hat{H}(s) = k s^{n_d - n_i} e^{-\tau s} \frac{\prod_{i=1}^{n_{z_1}} \left(s - a_{z_i}\right) \prod_{i=1}^{n_{z_2}} \left(s^2 + 2\zeta_{z_i}\omega_{z_i} s + \omega_{z_i}^2\right)}{\prod_{i=1}^{n_{z_1}} \left(s - a_{p_i}\right) \prod_{i=1}^{n_{z_2}} \left(s^2 + 2\zeta_{p_i}\omega_{p_i} s + \omega_{p_i}^2\right)} \tag{4}$$

using the following "elementary factors:" gain k, time delay τ, n_d pure differentiators, n_i pure integrators, n_{z_1} first-order zeros at the roots a_{z_i}, n_{p_1} first-order poles at the roots a_{p_i}, n_{z_2} second order zeros with frequencies ζ_{z_i} and natural frequencies ω_{z_i}, and n_{p_2} second order poles with frequencies ζ_{p_i} and natural frequencies ω_{p_i}. This parameterization allows the analyst to intuitively modify the model based on differences between the model and data frequency responses. Check boxes are placed for the gain, delay, differentiators, and integrators to include or discard these factors from the model. A combination of edit fields and sliders are provided for the gain and delay entries, whereas spinners are for the differentiators and integrators. As these values are changed, the Bode plots and differences are updated in real time, allowing the user to immediately see the affects of changing the model. Below are list boxes to provide first- and second-order zeros and poles. Depending on which type of factor is being changed, edit fields and sliders for either the root location or the damping ratio and natural frequency are highlighted. As the transfer function gain is correlated with most parameters, as discussed more below, a "Gain hold" button was added so that poles and zeros could be adjusted without wildly changing the overall gain of the model.

The "Fitting Metrics" panel on the far right contains various metrics the analyst can use in gauging the fit of the model to the frequency response data. The model residuals

$$v(j\omega_k) = H(j\omega_k) - \hat{H}(j\omega_k) \tag{5}$$

are the differences between the frequency response data and the model for that data. The first metric is the residual power spectral density, which is assumed to be constant with frequency [25] and can be estimated from the residuals as

$$\hat{S}_{vv} = \left(\frac{\pi}{\omega_{n_\omega} - \omega_1}\right) \sum_{k=1}^{n_\omega} |v(j\omega_k)|^2 \tag{6}$$

The factor in front of the summation accounts for the case when the entire spectrum up to the Nyquist frequency is not used, similar to Ref. [26]. Smaller residual covariances indicate a closer fit of the data. Another fitting metric is the coefficient of determination

$$R^2 = 1 - \frac{\sum_{k=1}^{n_\omega} |v(j\omega)|^2}{\sum_{k=1}^{n_\omega} |H(j\omega_k)|^2 - n_\omega \bar{H}\bar{H}^*} \tag{7}$$

where $\bar{\ }$ denotes the mean value. The R^2 quantifies the fit of the variation of the data by the model and ranges between 0 (no fit) and 1 (perfect fit). These fitting metrics are based on the complex-valued frequency response, and are independent of the method used to visualize the frequency response. Also shown in Fig. 1 are the maximum differences, quoted in dB of magnitude and deg of phase. All of these metrics update with changes in the model from the sliders or edit fields, and are available to the analyst to gauge the transfer function fit to the frequency response data.

B. Parameter Estimation

The "Fitting" tab is used to perform the optimization of the model parameters in Eq. (4), once the model structure and preliminary values are assigned by the analyst. This optimizes the available model parameters to achieve a better fit to the frequency response data and to provide modeling feedback through the estimated uncertainties. A screenshot is shown in Fig. 2.

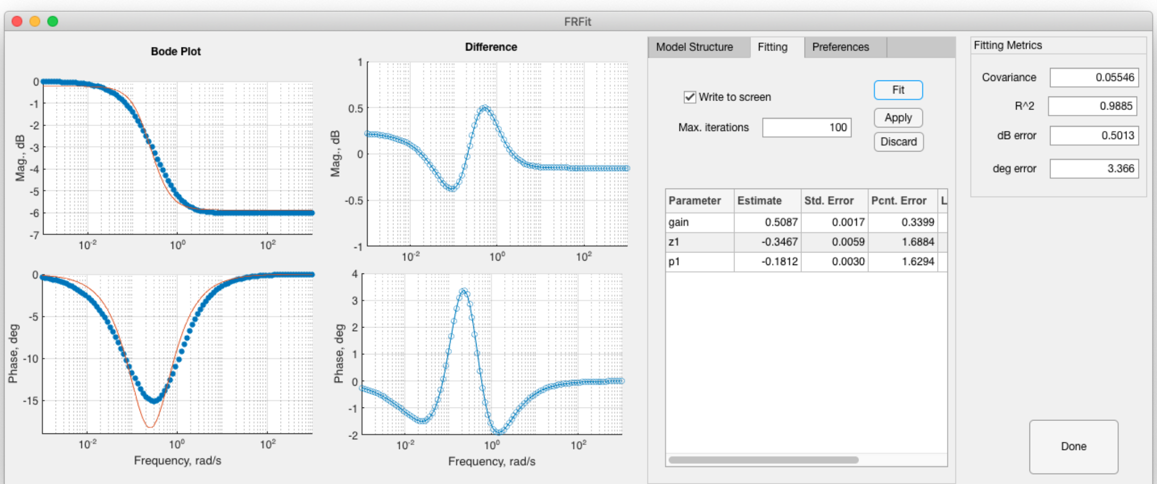

Fig. 2 FRFit fitting window.

The vector of unknown model parameters to be estimated, $\boldsymbol{\theta}$, includes any gain, delay, zeros, and poles included in the model structure. (Differentiators and integrators do not include model parameters to be estimated.) Because the model is parameterized as Eq. (4), determining the parameters is a nonlinear estimation problem. As such, a nonlinear optimization routine is used with the manually-tuned values as initial starting values. The optimization used is described in Refs. [2, 7, 25, 27] and briefly summarized here. Currently, software routines from Ref. [21] are called to perform the optimization.

The cost function used for estimating the parameters is the negative-log of maximum likelihood function, with the constant term removed, was

$$J(\boldsymbol{\theta}, S_{vv}) = \frac{n_\omega}{S_{vv}} \sum_{k=1}^{n_\omega} |v(j\omega_k)|^2 + n_\omega \ln\left(\frac{\pi S_{vv}}{n_\omega}\right) \tag{8}$$

Direct minimization of Eq. (8) is not well posed, so the unknown model parameters and error covariance matrix are optimized in an alternating manner, called a relaxation technique, while the other is held constant. When the model parameters are held constant, optimization of Eq. (8) with respect to S_{vv} is Eq. (6). Holding S_{vv} constant at this value, the model parameters are optimized by minimizing the cost function

$$J(\boldsymbol{\theta}) = \frac{n_\omega}{S_{vv}} \sum_{k=1}^{n_\omega} |v(j\omega_k)|^2 \tag{9}$$

which requires iteration using a nonlinear optimizer. For the Gauss-Newton method, the parameter update step is

$$\hat{\boldsymbol{\theta}} = \hat{\boldsymbol{\theta}}_0 - \mathbf{M}^{-1}\frac{\partial J}{\partial \boldsymbol{\theta}} \tag{10}$$

from the previous estimate $\hat{\boldsymbol{\theta}}_0$. In Eq. (10),

$$\mathbf{M} = \frac{2n_\omega}{S_{vv}} \Re\left[\sum_{k=1}^{n_\omega} \mathbf{S}^\dagger(j\omega_k)\,\mathbf{S}(j\omega_k)\right] \tag{11}$$

is the Fisher information matrix,

$$\frac{\partial J}{\partial \boldsymbol{\theta}} = -\frac{2n_\omega}{S_{vv}} \Re\left[\mathbf{S}^\dagger(j\omega_k)\,v(j\omega_k)\right] \tag{12}$$

is the local cost gradient, and

$$\mathbf{S}(j\omega_k) = \frac{\partial \hat{H}(j\omega_k)}{\partial \boldsymbol{\theta}} \tag{13}$$

is the frequency response sensitivity matrix. If the Gauss-Newton method diverges, a Simplex optimization routine is used to recover the estimate. However, if the model structure is sufficient for the data and the analyst has provided a reasonable fit to the data, this is usually not necessary.

In Eq. (13), the sensitivities can be computed using finite differences, or can be computed analytically. As discussed later in Section VI.A, the parameter estimates are correlated because a change in any of the parameters affects all outputs in similar ways over the frequency range of interest. Other parameterizations of the cost function yield different sensitivities [28]. However, if a model structure is over-parameterized, convergence issues will arise with any transfer function parameterization.

The optimization proceeds until the parameter estimates, cost function, cost gradient, and residual error covariance converge to within specified threshold values. The optimization also terminates if it reaches the user-specified maximum number of iterations. Intermediate results are printed to the command prompt if desired, so the user may monitor the optimization.

Afterwards, the uncertainties are calculated as

$$\mathrm{cov}(\hat{\boldsymbol{\theta}}) = \mathbf{M}^{-1} \tag{14}$$

which are the Cramér-Rao bounds. The parameter standard errors are the square-root of the diagonal terms in the parameter covariance matrix.

If prior information was included when FRFit was called, the above equations are modified as

$$J(\boldsymbol{\theta}) = \frac{n_\omega}{S_{vv}} \sum_{k=1}^{n_\omega} |v(j\omega_k)|^2 + n_\omega \left(\boldsymbol{\theta} - \boldsymbol{\theta}_p\right)^T \boldsymbol{\Sigma}_p^{-1} \left(\boldsymbol{\theta} - \boldsymbol{\theta}_p\right) \tag{15a}$$

$$\hat{\boldsymbol{\theta}} = \hat{\boldsymbol{\theta}}_0 - \mathbf{M}^{-1} \left[\frac{\partial J}{\partial \boldsymbol{\theta}} + \boldsymbol{\Sigma}_p^{-1} \left(\hat{\boldsymbol{\theta}}_0 - \boldsymbol{\theta}_p\right)\right] \tag{15b}$$

$$\mathbf{M} = \frac{2n_\omega}{S_{vv}} \Re \left[\sum_{k=1}^{n_\omega} \mathbf{S}^\dagger(j\omega_k)\,\mathbf{S}(j\omega_k)\right] + \boldsymbol{\Sigma}_p^{-1} \tag{15c}$$

where $\boldsymbol{\theta}_p$ and $\boldsymbol{\Sigma}_p$ are the prior estimates and covariance matrix. This option is available if prior information is known on some or all model parameters and should be included in the estimation. This can also be used to fix some parameters during the optimization. However, this option is not often used, as FRFit has been envisioned to be used with model structure determination problems.

Parameterizing the transfer function in terms of elementary factors can be more intuitive than specifying the orders of the numerator and denominator. In addition, it imposes an additional degree of structure on the model. For example, if the denominator was second order and the polynomial coefficients were estimated, the result could be either two real poles or a complex pair. In FRFit, because the parameters estimated would be either the two real pole locations or the damping ratio and natural frequency, the result would be consistent with the type of elements the user specified.

Once the parameter estimation has ended, the estimated parameters, standard errors, and percent errors are listed in the table. The user then has the option to use the estimated results, or discard them and return to the “Model Structure” tab.

C. Suggested Fitting Procedure

To build up the model structure, one approach is to fit the most prevalent features of the frequency response first, such as lightly damped second-order modes. The Bode magnitude plot provides most of the information on the model structure, and zeros can be used to disambiguate differences in phase. The differences plot is helpful for seeing what kinds of factors are needed to more closely match the modeling data. Another approach is to start at low frequencies, fitting the data as you move higher in frequency. The gain-hold feature is helpful in that the gain does not vary largely as other factors are added into the model and adjusted.

The time delay parameter is generally added last, as a final refinement of the model parameters and to fit additional phase lags due to time delays in the system, nonlinearities, and higher-order dynamics.

VI. Examples

A. F-16 Stabilator to Pitch Rate Simulation Data

This first example uses the F-16 nonlinear flight dynamics simulation included in SIDPAC to examine the stabilator to pitch rate transfer function. The simulation was trimmed for steady, wings-level flight at a 10,000 ft altitude and 5 deg angle of attack. A 120 s frequency sweep was applied to stabilator to excite the aircraft short period mode. The pitch rate was taken as output and measurement noise with standard deviation 0.2 deg/s was added. Frequency responses were computed between 0.2 and 7 rad/s from spectral densities using the binning approach [26], and frequencies with coherence below 0.8 were discarded, which resulted in data at 47 frequencies.

The data were loaded into FRFit. A gain of −13 and a second-order pole $[0.5, 2.2]$* were added and adjusted to fit the short-period resonance, giving $R^2 = 0$ and $S_{vv} = 255$. A first-order zero with a low break frequency was observable from the differences, so it was added as (-0.5) and the gain moved to −8, resulting in $R^2 = 0.93$ and $S_{vv} = 7.8$.

Optimizing these model parameters from these starting values converged in 14 iterations and resulted in the parameters listed in the last column of Table 1. The second column shows values obtained by linearizing the nonlinear simulation using central finite differences and truncating all states but the angle of attack and pitch rate. The third column are the manually-tuned values used to start the optimization. The optimized values are within one standard deviation of the linearized values. The standard errors are small, within 15%, for all parameters except for the first-order pole. The relative error on this parameter is high due to the few data points around the corner frequency of the factor.

*A short-hand notation is sometimes used in specifying first- and second-order poles and zeros. Values in parentheses indicate the negative root of a pole or zero. Values in brackets indicate damping ratio and natural frequency.

Table 1 Parameter estimates for the F-16 simulation example.

Parameter	True value	Initialized value $R^2 = 0.93$ $S_{vv} = 7.4$	Optimized value $R^2 = 0.99$ $S_{vv} = 1.2$
k	−6.4	−8.0	−6.8 ± 0.55 (8.1%)
a_{z_1}	−0.63	−0.5	−0.66 ± 0.22 (32%)
ζ_{p_1}	0.44	0.5	0.46 ± 0.050 (11%)
ω_{p_1}	2.1	2.2	2.1 ± 0.12 (5.6%)

Bode plots are shown in Fig. 3. The frequency response data used for modeling is shown as black dots. The linearized nonlinear simulation (full state and not truncated) is shown as the blue dashed line. The fitted model with parameters in the fourth column of Table 1 is the red line. This plot shows the modeling data showed an accurate depiction of the system dynamics, and that the fitted model fit this data well. The increased scatter in the frequency response data at higher frequencies is due to lower signal to noise, and some evidence of the phugoid mode is present in the linearized model at the lower frequencies.

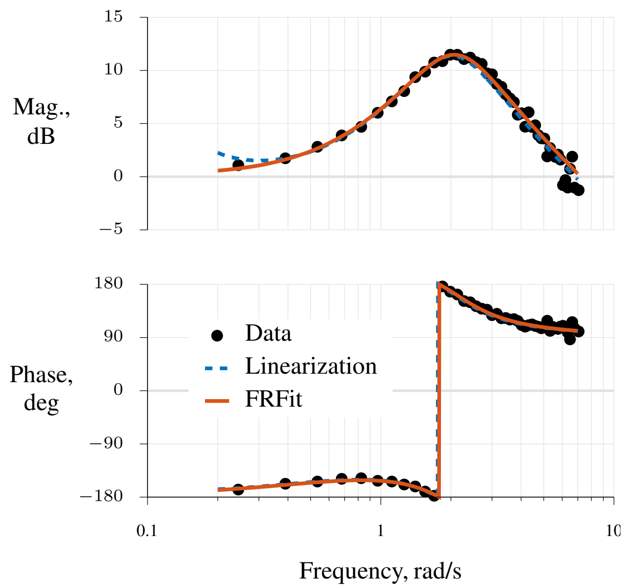

Fig. 3 Bode plot of elevator to pitch rate for the F-16 example.

The parameter-output sensitivities for the identified model, shown as Bode plots in Fig. 4, illustrate why using this model structure and only this single-input single-output frequency response data is a difficult optimization problem [28]. At low frequencies, all parameters except the damping ratio are correlated together because they are in phase. However, but the damping ratio is not as observable at low frequencies as it is near the short period resonance because of the low magnitude. A high frequencies, all parameters are correlated except for the gain. The gain sensitivity magnitude rolls off at 20 dB/dec less than the other sensitivities, but it may require higher-frequency data where the aircraft response has lower signal to noise or where other dynamics exist. All parameters have the strongest sensitivity at the short period resonance, but the gain and damping ratio are correlated, as are the zero and natural frequency. This is one reason why it is important to use a range of frequencies for identification, and motivates using additional input and output measurements. It is also apparent that the zero has strong sensitivity at the lower frequencies, where the data is more sparse, though it is correlated with other parameters.

This example was included to show the general fitting procedure, illustrate that the optimized model parameter estimates are in statistical agreement with the known solution, and show the effect of the frequency response sensitivities.

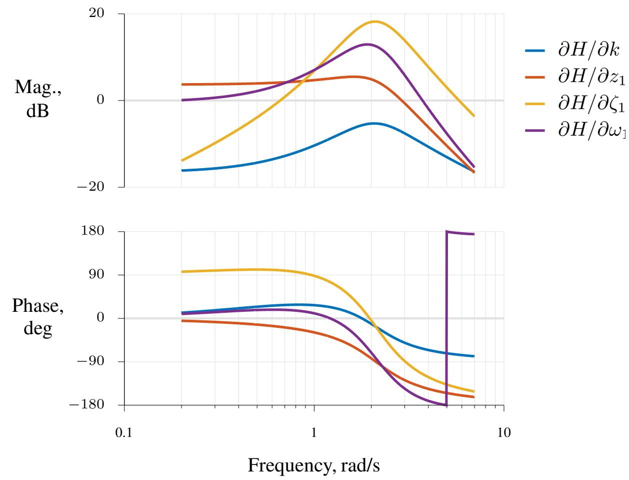

Fig. 4 Bode plot of elevator to pitch rate frequency response sensitivity functions for the F-16 example.

B. DC-3 Elevator to Pitch Angle Flight Data

Frequency response data for the elevator to pitch angle transfer function of a DC-3 airplane flying at 7500 ft and 220 ft/s is given as a Bode plot in Fig. 14.1 of Ref. [19]. These data were digitized and are shown in Fig. 5 as black dots. Six data points were omitted because both magnitude and phase information were not present. Although care was taken in the digitization process, small errors may have been inadvertently added to these data.

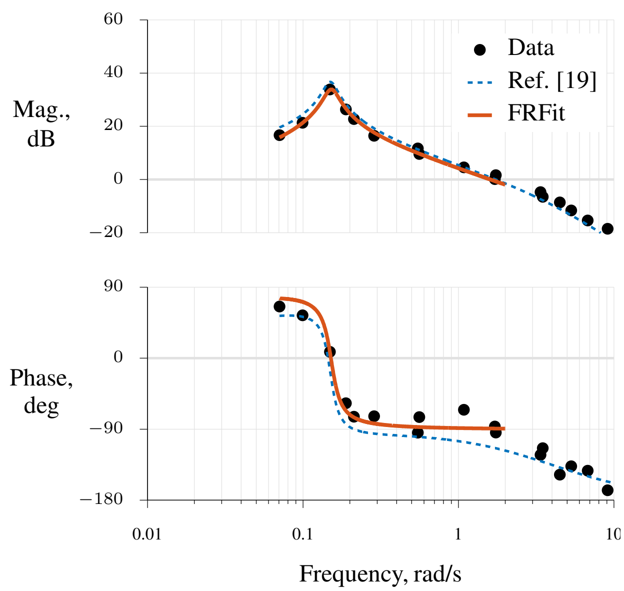

Fig. 5 Bode plot of elevator to pitch angle for the DC-3 example.

After an iterative manual tuning procedure, Ref. [19] suggests the transfer function

$$H(s) = \frac{7.5(s + 0.021)(s + 0.067)(s + 0.15)}{(s + 0.14)(s + 0.46)(s + 4)[s^2 + 2(0.10)(0.15)s + (0.15)^2]} \tag{16}$$

as a sufficient fit to the data*. As traditional models for this transfer function include two first-order zeros and two second-order poles [29], Eq. (16) appears to be over-parameterized. Although this transfer function fits the data well

*For consistency, a different factorization of the transfer function is given in Eq. (16) than appears in Ref. [19]. The gain was also changed from 11 to 7.5 to fix a suspected typo in Ref. [19].

(R^2 = 0.62 and S_{vv} = 1120), attempts to further improve the model parameters were unsuccessful, as the optimization would not converge. Upon exiting the optimization, some of the weaker parameters had shifted significantly and most of the parameters had errors above 200%, which indicated they were not statistically important and should be removed from the model structure. Other parameterizations of Eq. (16) and also other estimation techniques led to poor fits, providing further evidence of an over-parameterized model. As the data shown in Ref. [19] came from an unpublished work [30], it is difficult to obtain further evidence supporting this model structure.

Using FRFit, a gain of 0.3 and second-order pole $[0.05, 0.15]$ was first added to fit the low-frequency phugoid resonance. The low-frequency errors below 2 rad/s had a 20 dB/dec slope and a 90 deg phase change, so a first-order zero was added. The zero was then added and adjusted to (0.04) and the gain to 1.5 to flatten the low-frequency differences and shift the magnitude differences. Optimizing this model for the data converged within 16 iterations, fit the low-frequency data well (R^2 = 0.99 and S_{vv} = 33), and produced a reasonable parameters. However, the first-order zero had errors of over 190% due to the lack of low-frequency data.

To attempt to fit the higher-frequency resonance at the short period mode, a second-order pole was at $[0.6, 7]$ and a first-order zero at (9) were added, and the gain was adjusted to 7.3. The data fit well using this classical model structure (R^2 = 0.99 and S_{vv} = 32), but the optimization could not converge. Also, almost all error bounds were on the order of 100%.

Finally, the attempt to model the short period mode was abandoned, and the frequency range of the model was restricted to the 11 data points between 0.7 to 2.0 rad/s to discard the higher-frequency magnitude and phase changes from the short period mode. The phugoid approximation including the first-order zero and second-order pole was rerun over this range using the same starting parameters. The optimization again converged to approximately the same values in 16 iterations. Standard errors were slightly larger than using the entire frequency range of data. Parameters and standard errors are listed in Table 2. The uncertainty for the first-order zero remained large. The red line in Fig. 5 shows the fitted model over the restricted frequency range. Parameters were reasonable.

Table 2 Parameter estimates for the DC-3 example.

Parameter	Initialized value	Optimized value
	$R^2 = 0.00$	$R^2 = 0.99$
	$S_{vv} = 3335$	$S_{vv} = 32$
k	1.5	1.6 ± 0.42 (27%)
a_{z_1}	−0.04	-0.0087 ± 0.041 (466%)
ζ_{p_1}	0.05	0.11 ± 0.033 (31%)
ω_{p_1}	0.15	0.15 ± 0.0051 (3.3%)

Had not conventional dynamics of the subject dynamics been already known, a pure differentiator would have worked well for this data set in place of the first-order zero. Removing the first-order zero, replacing it with a pure differentiator, and optimizing the remaining model parameters converged in 14 iterations to approximately the same results as listed in Table 2. The fit was still good (R^2 = 0.99, S_{vv} = 36), but the uncertainties in the gain and damping ratio increased slightly.

This example was included to show how it can be difficult to obtain a unique transfer function for a given set of data, how a model can be overfit, and the important role of physical insight in modeling. An interactive process, such as that used in FRFit, can be helpful. Although the effect of the low-frequency first-order zero could be seen on the modeled data, improvements in its estimate would benefit from additional low-frequency data near its corner frequency. Estimates of the higher-frequency short period mode, of which the models differed, would benefit from looking at other measurement data, such as a rate gyroscope or a vertical accelerometer. Because the data were given as a Bode plot, other identification techniques based on time histories or Fourier transforms of input and output data were not applicable to this problem.

C. Approximation of Theodorsen's Function

In the unsteady aerodynamic theory of Theodorsen [31], the aerodynamic forces are given in terms of noncirculatory (apparent mass) effects and circulatory effects. The circulatory contributions are multiplied by a frequency-dependent factor called Theodorsen's function $C(k)$, where k is the reduced frequency. The function is complex-valued and defined as

$$C(k) = \frac{H_1^{(2)}(k)}{H_1^{(2)}(k) + jH_0^{(2)}(k)} \tag{17}$$

with the Hankel functions

$$H_v^{(2)}(k) = J_v(k) - jY_v(k) \tag{18}$$

where J_v and Y_v are Bessel functions of the first and second kind, respectively [32].

Theodorsen's function is therefore a frequency-dependent transfer function. However, it is not easily expressed in terms of polynomial transfer functions or elementary factors. Indeed, several works have considered many approximations of various transfer function orders, as summarized in Ref. [33]. All of these transfer functions have the same number of poles as zeros so that the magnitude is flat for low- and high-frequency asymptotes, resulting in n/n-type transfer function models with relative degree 0.

To investigate using FRFit, Theodorsen's function was evaluated using Eq. (17) for 100 reduced frequencies, equally spaced between $k = 10^{-3}$ and $k = 10^3$. A pole and zero were placed to form a 1/1-type transfer function, and those values along with the gain were manually tuned to approximate Theodorsen's function. These values are the second column in Table 3 and the dashed line in Fig. 6(a). Optimizing this model used 18 iterations and led to the parameters in the third column of Table 3 and the solid red line in Fig. 6(a). The fit to the theory was closer, but significant differences in the magnitude and phase remained.

To obtain a higher-order fit, two zeros and two poles were used next, as a 2/2-type transfer function. Instead of manually tuning these parameters, Jones' approximation was used [32–34]. Running the optimization used 26 iterations for convergence and improved the fit and lowered the residual covariance, slightly. These values are given in Table 4 and Bode plots are shown in Fig. 6(b). Only small differences in the Bode plots are evident.

Table 3 Parameter estimates for the Theodorsen function example.

Parameter	Initialized value	Optimized value
	$R^2 = 0.87$	$R^2 = 0.99$
	$S_{vv} = 0.62$	$S_{vv} = 0.055$
k	0.50	0.51 ± 0.0017 (0.34%)
a_{z_1}	−0.22	-0.35 ± 0.0059 (1.7%)
a_{p_1}	−0.13	-0.18 ± 0.0030 (1.6%)

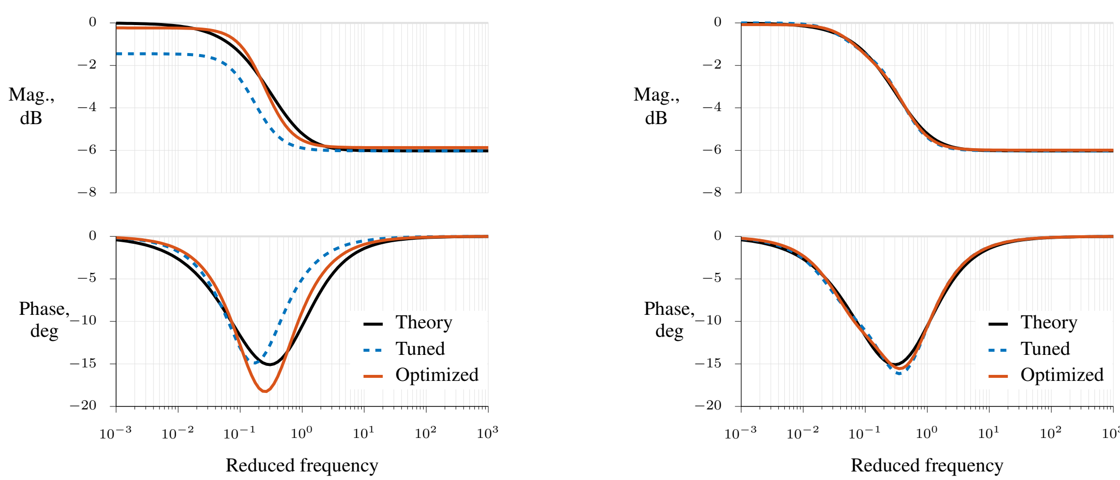

(a) 1/1-type transfer function.

(b) 2/2-type transfer function.

Fig. 6 Bode plots of approximations to Theodorsen's function.

Table 4 Parameter estimates for the Theodorsen function example.

Parameter	Initialized value [33, 34]	Optimized value
	$R^2 = 1.00$	$R^2 = 1.00$
	$S_{vv} = 0.0059$	$S_{vv} = 0.0035$
k	0.50	$0.50 \pm 0.0005\,(0.091\%)$
a_{z_1}	−0.054	$-0.077 \pm 0.0019\,(2.5\%)$
a_{z_2}	−0.51	$-0.54 \pm 0.0056\,(1.0\%)$
a_{p_1}	−0.046	$-0.063 \pm 0.0013\,(2.1\%)$
a_{p_2}	−0.30	$-0.33 \pm 0.0047\,(1.4\%)$

Higher-order transfer functions were also attempted. For example, Ref. [33] provides transfer functions for 3/3- and 4/4-type transfer functions. However, even with the starting values provided, the optimization would not converge on a solution, which indicates those models are over-parameterized for a parameter estimation problem.

D. Reduced-Order Modeling of CFD Data

This section will include a single-input single-output example from Ref. [1].

VII. Conclusions

This paper describes a program designed for fitting a transfer function to frequency response data. As determining the model structure for a model can be tedious and time consuming, the program was designed to be interactive, so the analyst can quickly update the model structure through transfer function "elementary factors" added and modified using buttons, sliders, and edit fields to see the results change in real time. A maximum likelihood estimator is also included which can refine manually-tuned estimates.

The program was written in MATLAB® using the App Designer™. The program is small and versatile, and can be reengineered from the present description. The software is planned for public release on the NASA Software Catalog to U.S. citizens.

The main benefit of the program comes from examining data for complicated systems, for one frequency response at a time, to assess the structure of the model. The interactive nature of the program can speed up the analysis, which would otherwise entail programming optimizations in a time-consuming trial and error fashion. The program can also serve as a teaching aid due to its real time and interactive ability.

The program is limited to frequency response data (provided by the analysis), single-input single-output transfer function models, and linear systems. However, information gathered from using FRFit can be applied in more complicated parameter estimations using other software with many inputs and many outputs.

Acknowledgments

This research was supported by the NASA Advanced Air Transport Technology (AATT) Project.

References

[1] Grauer, J., Waite, J., and Stanford, B., "Reduced-Order Aerodynamic Modeling Based on CFD Frequency Responses from Multisine Inputs," Submitted to AIAA SciTech Forum, 2021.

[2] Grauer, J., and Boucher, M., "Aircraft System Identification from Multisine Inputs and Frequency Responses," AIAA Paper 2020-0287, 2020. doi:10.2514/6.2020-0287.

[3] Tischler, M., and Remple, R., *Aircraft and Rotorcraft System Identification: Engineering Methods with Flight Test Examples*, 2nd ed., AIAA, Reston, VA, 2012. doi:10.2514/4.868207.

[4] Klyde, D., and Schulze, P., "Determining Handling Qualities Parameters: Lessons from the Frequency Domain," AIAA Paper 2020-0508, 2020. doi:10.2514/6.2020-0508.

[5] Ljung, L., *System Identification*, Prentice Hall, Upper Saddle River, NJ, 1999.

[6] Murray, J., and Maine, R., "pEst Version 2.1 User's Manual," NASA TM-88280, September 1987.

[7] Morelli, E., and Klein, V., *Aircraft System Identification: Theory and Practice*, 2nd ed., Sunflyte, Williamsburg, VA, 2016.

[8] anon., "NASA Software Catalog," `https://software.nasa.gov`, accessed May 2020.

[9] James, H., Nichols, N., and Phillips, R., *Theory of Servomechanisms*, McGraw-Hill, New York, NY, 1947.

[10] Seamans, R., Bromberg, B., and Payne, L., "Application of the Performance Operator to Aircraft Automatic Control," *Journal of the Aeronautical Sciences*, Vol. 15, No. 9, 1948, pp. 535–555. doi:10.2514/8.11644.

[11] Grauer, J., and Morelli, E., "Method for Real-Time Frequency Response and Uncertainty Estimation," *Journal of Guidance, Control, and Dynamics*, Vol. 37, No. 1, 2014, pp. 336–343. doi:10.2514/1.60795.

[12] Grauer, J., and Boucher, M., "Real-Time Estimation of Bare-Airframe Frequency Responses from Closed-Loop Data and Multisine Inputs," *Journal of Guidance, Control, and Dynamics*, Vol. 43, No. 2, 2020, pp. 228–298. doi:10.2514/1.G004574.

[13] Bendat, J., and Piersol, A., *Random Data: Analysis and Measurement Procedures*, 2nd ed., John Wiley & Sons, New York, NY, 1986.

[14] Juang, J., *Applied System Identification*, Prentice Hall, Upper Saddle River, NJ, 1994, pp. 121–274.

[15] Silva, W., "AEROM: NASA's Unsteady Aerodynamic and Aeroelastic Reduced-Order Modeling Software," *Aerospace*, Vol. 5, No. 41, 2018, pp. 1–18. doi:10.3390/aerospace5020041.

[16] Pintelon, R., and Schoukens, J., *System Identification: A Frequency Domain Approach*, 2nd ed., John Wiley & Sons, Hoboken, NY, 2012.

[17] Bode, H., *Network Analysis and Feedback Amplifier Design*, D. Van Nostrand Company, New York, NY, 1945, pp. 337–359.

[18] Lees, S., "Graphical Aids for the Graphical Representation of Functions of the Imaginary Argument," MIT Engineering Memorandum E-25, February 1951.

[19] Bruns, R., and Saunders, R., *Feedback Control Systems*, McGraw-Hill, New York, NY, 1955, pp. 291–313.

[20] Batterson, J., "STEP and STEPSPL — Computer Programs for Aerodynamic Model Structure Determination and Parameter Estimation," NASA TM-86410, January 1986.

[21] Morelli, E., "System IDentification Programs for AirCraft (SIDPAC)," version 4.1, NASA Software Catalog, `http://software.nasa.gov`, accessed May 2020.

[22] Levy, E., "Complex-Curve Fitting," *IRE Transactions on Automatic Control*, Vol. AC-4, No. 1, 1959, pp. 37–43. doi:10.1109/TAC.1959.6429401.

[23] Morelli, E., "Transfer Function Identification using Orthogonal Fourier Transform Modeling Functions," AIAA Paper 2013-4749, 2013. doi:10.2514/6.2013-4749.

[24] Sanathanan, C., and Koerner, J., "Transfer Function Synthesis as a Ratio of Two Complex Polynomials," *IEEE Transactions on Automatic Control*, Vol. 8, No. 1, 1963, pp. 56–58. doi:10.1109/TAC.1963.1105517.

[25] Grauer, J., "Dynamic Modeling using Output-Error Parameter Estimation based on Frequency Responses Estimated with Multisine Inputs," NASA TM-2018-220108, November 2018.

[26] Morelli, E., and Grauer, J., "Practical Aspects of Frequency-Domain Approaches for Aircraft System Identification," *Journal of Aircraft*, Vol. 57, No. 2, 2020, pp. 268–291. doi:10.2514/1.C035599.

[27] Klein, V., "Aircraft Parameter Estimation in Frequency Domain," AIAA Paper 78-1344, 1978. doi:10.2514/6.1978-1344.

[28] Morelli, E., "Identification of Low Order Equivalent System Models From Flight Test Data," NASA TM-2000-210117, August 2000.

[29] McRuer, D., Graham, D., and Ashkenas, I., *Aircraft Dynamics and Automatic Control*, Princeton University Press, Princeton, NJ, 1973, pp. 296–352.

[30] Schuck, O., "Application of Theory to the Practical Design of Airplane Controls," unpublished paper presented to AIEE Conference on Feedback Control Systems, 1951.

[31] Theodorsen, T., "General Theory of Aerodynamic Instability and the Mechanism of Flutter," NACA Report No. 496, January 1949.

[32] Leishman, J., *Principles of Helicopter Aerodynamics*, Cambridge University Press, New York, NY, 2006, pp. 423–440.

[33] Brunton, S., and Rowley, C., "Empirical State-Space Representations for Theodorsen's Lift Model," *Journal of Fluids and Structures*, Vol. 38, 2013, pp. 174–186. doi:10.1016/j.jfluidstructs.2012.10.005.

[34] Jones, R., "Operational Treatment of the Nonuniform-Lift Theory in Airplane Dynamics," NACA Technical Note No. 667, October 1938.